Journal of the Korean Nuclear Society
Volume 32, Number 3, pp.214~226, June 2000

MARS/MASTER Solution to OECD Main Steam Line Break Benchmark Exercise III

Jae-Jun Jeong, Han Gyu Joo, Bub Dong Chung, Kwi Seok Ha, Won Jae Lee, Byung-Oh Cho, and Sung-Quun Zee

Korea Atomic Energy Research Institute
150 Dukjin-dong, Yusong-gu, Taejon 305-353, Korea
jjjeong@kaeri.re.kr

(Received October 29, 1999)

Abstract

In an effort to assess the performance of KAERI' s coupled 3D kinetics - system T/H code, MARS/MASTER, Exercise III of the OECD main steam line break benchmark is solved. The analysis model of the reference plant, TMI-1 - a 2772 MWth B&W plant, consists of three major components: a core neutronics model involving 241x28 neutronic nodes, a vessel 3D T/H model consisting of 374 hydrodynamic volumes, and a 1D system T/H model containing 157 hydrodynamic volumes. The results show that there is a significant amount of flow mixing occurring in the upper and lower plenum regions and the core power distribution evolves to a highly localized shape due to the presence of a stuck rod, as well as the asymmetric flow distribution. It is judged that MARS/MASTER properly captures these drastic 3-dimensional effects. Comparisons with other results submitted to OECD confirm the accuracy of the MARS/MASTER solution.

Key Words : coupled 3D kinetics - system T/H code, MARS/MASTER, steam line break, OECD MSLB benchmark, retrun-to-power

1. Introduction

MARS/MASTER is a coupled three-dimensional neutron kinetics/system thermal-hydraulic (T/H) code developed at the Korea Atomic Energy Research Institute (KAERI) for best-estimate safety analyses. Compared to the conventional system codes employing lower dimensional models, e.g. point kinetics with one-dimensional T/H model, the coupled system codes are expected to provide substantially more accurate predictions in the analysis of the system transients involving strong interactions between neutronic and T-H phenomena. This is because that a realistic representation of the physical system in the three-dimensional space reduces the errors associated with the assumptions introduced in the lower dimensional models.

One of the assumptions made in using a point kinetics model is that the reactivity change during the transient can be properly represented by a few sets of reactivity coefficients. However, the validity of the reactivity coefficients, which are to be generated from a set of steady-state neutronic calculations, is not guaranteed in the transient situations in which the actual core condition is far from the conditions for which the reactivity coefficients are generated. The most practical problem in this regard is the possibility of a return-to-power in a steam line break problem. A point kinetics model may predict a return-to-power while a three-dimensional kinetics model does not. As far as predictions of local safety parameters are concerned, the point kinetics models result in too conservative results due to their inability to adapt to the changes in the neutron flux shape. It is expected that the coupled codes can significantly reduce the conservatism of the lower dimensional models.

In order to assess the performance of a coupled code, one needs a test problem in which severe three-dimensional changes in the neutron flux as well as flow and temperature distributions occur during the transient. The steam line break accident, which results in increased heat removal in one of the coolant loops, is one good such test problem in that it involves a considerable imbalance in the flow condition as well as strongly skewed radial power distributions due to the assumption of a stuck rod.

The OECD main steam line break (MSLB) benchmark problem [1] was established in this regard in December 1996 and numerous institutions worldwide submitted solutions generated with their own coupled codes. KAERI participated in this benchmark with the MARS/MASTER code in order to assess the overall performance of the code. The work here is to present the analysis models and results for Exercise III of the benchmark and then to compare with the results of other participants.

In the following section, a brief description of the MARS/MASTER coupled code is given to provide a general understanding of the code' s capability, employed methods and the coupling scheme. It is followed by a description of the benchmark problem that defines the specifications and the transient scenario. The MARS/MASTER analysis models are then described in Section 4 with emphases made on the three-dimensional fluid modeling. In Section 5, the primary results of interest are presented and discussed.

2. The MARS/MASTER Code

The MARS/MASTER code was developed by integrating two independent codes, MARS [2-4] and MASTER [5]. MARS is a multi-dimensional system thermal-hydraulic code developed for best-estimate analyses of two-phase thermal-hydraulic transients in light water reactors. The backbones of the MARS code are the RELAP5/MOD3 and COBRA-TF codes developed by the USNRC, and they provide the bases of the one-dimensional (1D) and three-dimensional (3D) modules of MARS, respectively. The 3D module is used for a realistic representation of the thermal-hydraulic field within the reactor vessel whereas the 1D module is used for the rest of the system. The coupling of the 1D and 3D module hydrodynamic models is resolved by solving an implicitly-coupled system pressure matrix equation. Since MARS retains the unique features of the two base codes, it is as versatile and robust as RELAP5 while it allows multi-dimensional nodalization schemes as COBRA-TF. The real value of the MARS code is the enhanced solution accuracy attainable with realistic modeling. In addition, MARS has superb user-friendliness achieved by the Windows graphic feature.

MASTER is a two-group, three-dimensional neutron diffusion code capable of microscopic depletion, xenon dynamics, on-line DNB analysis, and kinetics calculation in both rectangular and hexagonal geometries. The primary neutronic solver of the MASTER code is the nodal expansion/integration method (NEM/NIM) formulated within the framework of the coarse-mesh rebalancing technique. As optional solvers, it has also the analytic function expansion nodal (AFEN) method, as well as the nonlinear analytical nodal method (ANM) solvers. The transient thermal-hydraulic solution in MASTER is achieved by the COBRA III-C/P module, which employs the homogeneous equilibrium model. The mapping between the neutronic and T/H nodes is basically one-to-one. The COBRA module provides MASTER with the features of cross flow modeling and subchannel analysis on the fly. The types of transient calculations that can be analyzed by the MASTER code include control rod perturbation (ejection, withdrawal and drop), flow perturbation (steam line break), and boron dilution events.

The coupling of MARS and MASTER was achieved under the Windows operating system so that the use of the dynamic link library (DLL) feature could be used and the code can be executable on personal computers [6]. The use of DLL allowed maintaining the integrity of each code independently as well as keeping simpler coupled code structures. Only minor coding changes were needed for data communication and for incorporating feedback data, leaving the majority of the codes intact. In the coupled mode, the transient core T/H conditions characterized by the coolant density and effective fuel temperature distributions are determined at each time step by MARS and transferred to MASTER so that they can be used to update the group constants. The power distribution newly obtained by MASTER is then sent back to MARS for the T/H calculation at the next time step. Thus, the COBRA-IIIC/P roles in the original MASTER are completely replaced with MARS in the coupled code system. The data communication is achieved through a common memory area, which is shared by both codes.

3. The OECD MSLB Benchmark

The steam line break accident involves significant overcooling in one of the cold legs due to rapid depressurization in the affected steam generator. If the break occurs at the front of the main steam isolation valve, evaporation continues until the pressure of the affected steam generator equals the containment pressure. Because only one loop is overcooled, considerable asymmetry occurs in the core inlet flow/temperature distributions that would cause an asymmetric radial power distribution through the thermal feedback effects. Moreover, the assumption of a stuck rod adds conservatism, drastically deteriorating the radial power distribution so that very high power peaks occur to cause local fuel damages. The OECD MSLB benchmark deals with such a severe transient for which the proper incorporation of 3D effects is important in both neutronic and T/H modeling.

The reference plant for this benchmark problem is TMI-1, a B&W designed pressurized water reactor. The rated power of this plant is 2772 MW_{th} and the coolant system is characterized by two hot legs, four cold legs, and two once-through type steam generators. Two steam nozzles are attached to each steam generator and the four steam lines are connected to a common header leading steam to the turbine. The reactor core consists of 177 fuel assemblies which are 357.12 cm long. The specifications [1] provide all the data needed for the neutronic and T/H modeling. The group constant data consisting of 438 unrodded

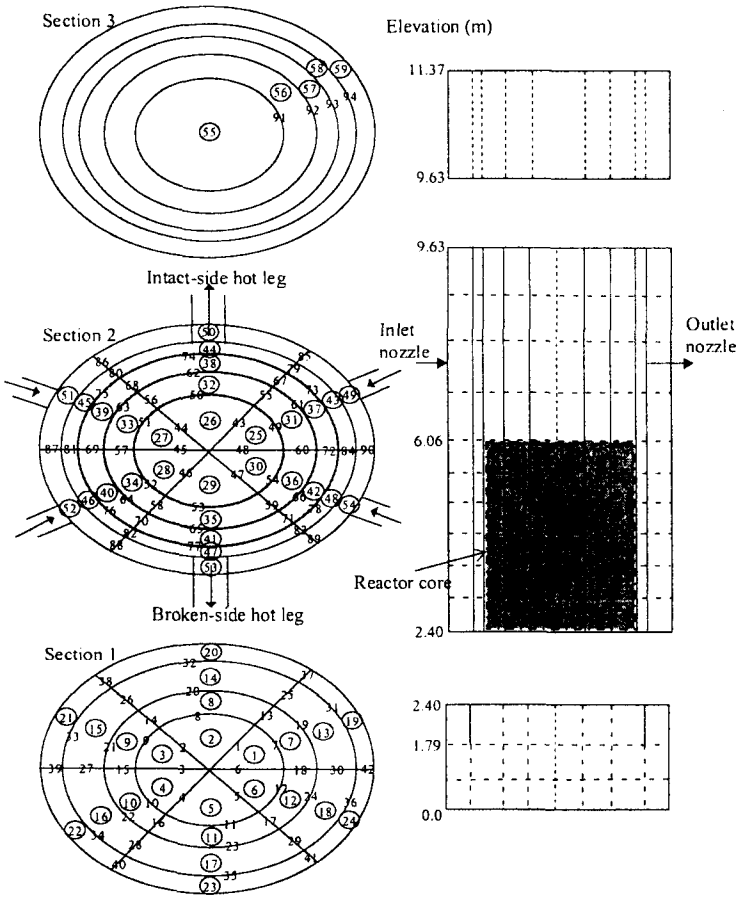

Fig. 1. TMI-1 Reactor Vessel and MARS 3D Model Nodialization

and 192 rodded group constant tables represent an end-of-cycle core. Regarding the control rod worth, two rodded group constant sets were provided in the specification: the best-estimate and the return-to-power ones. As far as the combination of neutronic and T/H modeling is concerned, there are three exercises defined in the benchmark:

(1) Exercise I - Point kinetics plant simulation:

The purpose of this exercise is to test the primary and secondary system model response. The compatible point kinetics model inputs, which preserve the axial and radial power distributions and tripped rod reactivity from Exercise III, are provided.

(2) Exercise II - Coupled 3D neutronics/core thermal-hydraulics response evaluation:

The purpose of this exercise is to model the core and the vessel only. Inlet and outlet core transient boundary conditions are provided.

(3) Exercise III - Best-estimate coupled core/plant transient modeling:

This exercise combines elements of the first two exercises in this benchmark and is an analysis of this transient in its entirety.

KAERI analyzed Exercise II using both the MASTER code alone and the MARS/MASTER coupled code, and demonstrated that the T/H to neutronic mapping scheme is an important issue in local power predictions [7]. In the work here,

Exercise III with the rodded group constant set are analyzed. The initial condition for the transient is a hot-full-power state slightly rodded with a regulating bank. The steady-state conditions defined by the specification are summarized in Table 1 along with those established by the MARS/MASTER initialization run. The transient occurs at time 0.01 sec by assuming a double-ended break in a 24″ pipe and a slot break in an 8″ pipe. The reactor coolant pumps continuously operate during the transient. The control actions to occur are (1) reactor scram due to either over-power (114% with 0.4 sec delay) or low pressure (1935 psia with 0.5 sec delay), (2) steam isolation valve closure following the reactor trip, (3) high pressure injection (1645 psia with 25 sec delay). The transient is analyzed for a period of 100 seconds.

4. MARS/MASTER Analysis Models

The thermal-hydraulic behavior within the TMI-1 reactor vessel is modeled using the MARS 3D module. Figure 1 shows MARS 3D module nodalization for the reactor vessel. It consists of 3 sections, 59 channels, and 94 gaps (resulting in a total of 374 computational volumes). Each section in Figure 1 represents:

(1) Section 1 - lower downcomer and lower plenum below the bottom of the active core,
(2) Section 2 - upper downcomer, active core, core bypass, and upper plenum, and
(3) Section 3 - upper head.

The channels in the outer shell of Sections 1 and 2 represent the downcomer. Because the four cold legs and two hot legs are connected symmetrically to the reactor vessel, six circumferential meshes were used for the whole vessel. The hot legs are connected to the reactor vessel via cells (44,8) and (47,8), whereas the cold legs via cells (49,8), (51,8), (52, 8), and (54,8), where the first number in the parenthesis is the channel number and the second is the axial mesh number.

The active core is modeled using 18 flow channels (channels 25 through 42) and 6 axial meshes in Section 2. Each of the channels contains a heat structure to model average fuel rods in the channel. The gap conductance of the fuel rods is given as a constant (11356 W/m^2-K). The local power generation rates of the average fuel rods are determined by MASTER and transferred to MARS.

The neutronic nodalization in the MASTER model consists of 241 radial nodes (177 fuel nodes, each representing a fuel assembly, and 64 reflector nodes) and 28 axial nodes, most of which are equally spaced with a node size of 14.88 cm. A comparison of the thermal-hydraulic and neutronic meshes is given in Figure 2. Because of the different node structures, a mapping scheme was established to provide correspondences between neutronic and T/H meshes. As can be identified in Figure 2, the radial mapping scheme assigns about 10 neutronic nodes to a T/H node while about 4 axial neutronic nodes are assigned to a T/H node.

The primary coolant loops, steam generators, and steam lines are modeled using the MARS 1D module. The nodalization consists of 157 hydraulic volumes and 156 junctions as shown in Figure 3. Because a double-ended break of the 24-inch steam line and a slot break of the 8-inch pressure balance line should be specified in this transient, each steam line, connected to the broken-side steam generator, is modeled individually. However, the steam lines from the intact loop are lumped into a pipe component. To simulate primary-to-secondary heat transfer, a heat structure model is established for each steam generator. The "heat exchanging" region of the steam generators is divided into 12 equal-length

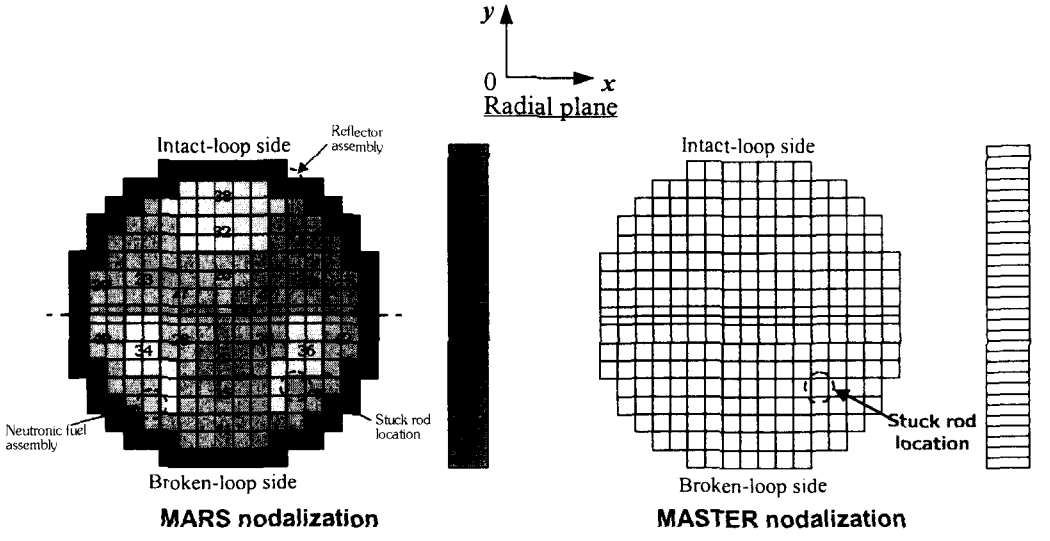

Fig. 2. Thermal-hydraulic and Neutronic Meshes for the Reactor Core

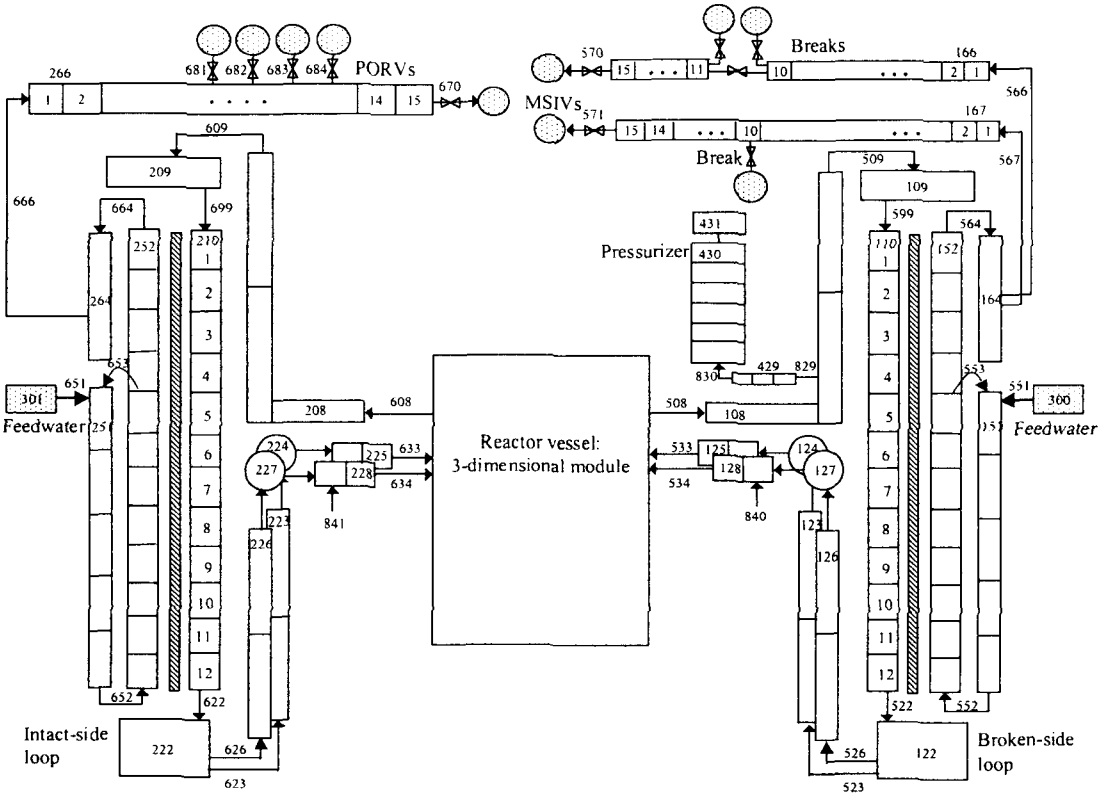

Fig. 3. MARS One-dimensional Module Nodalization for TMI-1 System

Table 1. Steady-state Conditions of the OECD MSLB Benchmark Problem

Parameter	Spec. Value	MARS/MASTER
Core Power, MW	2772.0	2772.0
RCS cold leg temperature, K	563.76	563.9
RCS hot leg temperature, K	591.43	591.9
Lower plenum pressure, MPa	15.36	15.37
Outlet plenum pressure, MPa	15.17	15.15
RCS pressure, MPa	14.96	14.96
Total RCS flow rate, kg/s	17602.2	17606.2
Core flow rate, kg/s	16052.4	16052.2
Bypass flow rate, kg/s	1549.8	1557.9
Pressurizer Level, m	5.59	5.599
Steam Flow per OTSG, kg/s	761.59	761.59
OTSG outlet pressure, MPa	6.41	6.41
OTSG outlet temperature, K	572.63	569.1
OTSG superheat, K	19.67	16.0
Initial SG inventory, kg	26000	27475.0
Feedwater temperature, K	510.93	510.93

vertical volumes. Other heat conductors are not taken into account as specified in the final specifications [1]. The two hot legs and four cold legs are modeled separately.

In summary, the reactor vessel is modeled with 374 hydrodynamic volumes by the MARS 3D module, other systems with 157 hydraulic volumes by the MARS 1D module, and the reactor core with (241 × 28) neutronic meshes by MASTER.

5. Analysis Results

It should be noted that the OECD MSLB Benchmark III is a hypothetical accident. Therefore there is no true solution established and the solutions generated by the participants reveal a wide band of variation [8]. There are numerous factors causing these differences. For instance, some codes such as MARS and TRAC, use a 3D T/H formulation for the reactor vessel whereas others use a 1D T/H formulation, and some uses much a coarser T/H nodalization in the core than the others. Hence, the evaluation of a solution is possible only through first examining the degree of modeling sophistication and then identifying the causes for the differences noted during the comparison. However, the full set of the other participants' detailed solutions is not available and only the total core power change data of about 10 participants are available [8]. Thus the comparison with other solutions is made only for the core power behavior. In the following, the MARS/MASTER results are given and their physical significances are discussed.

5.1. Steady-State Results

To establish a steady state, the following steps were carried out:

(1) A steady-state flow distribution in the three-dimensional reactor vessel is first obtained from a null transient calculation for the vessel only without the heat source in the reactor core.

(2) After reaching a steady-state flow, a null transient for the reactor vessel is calculated with the heat source; the power shape is

Table 2. Major Sequence of Events

Event description	Time (s)
Break opens	0.010
Trip on high neutron flux	5.958
Rod insertion begins	6.358
Turbine valves close completely	6.858
High pressure safety injection starts	36.67
Peak power occurs	67.30
Transient ends	100.0

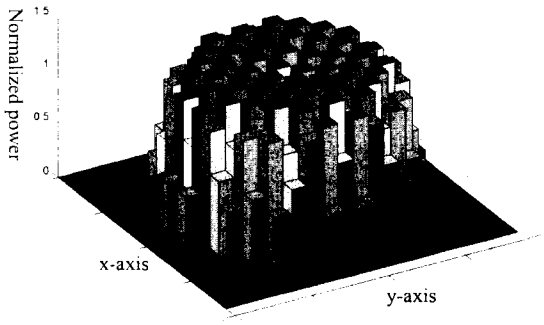

Fig. 4. Steay-state, Radial Power Distribution

obtained from MASTER. The coupled calculation is continued until the energy balance across of the reactor vessel reached a quasi steady state.

(3) A null transient for the whole system including the reactor vessel is then calculated, until a steady state is attained. This procedure is performed by the automatic initialization function of the MARS 3D module [4].

Table 1 compares the initial, steady-state conditions of the MARS/MASTER run with the final specifications. The results show good agreement except for the steam generator secondary-side inventory. The secondary-side inventory of a once-through steam generator is a function of pressure, temperature, flow, etc. As can be seen in Table 1, all these parameters agree well with the reference data. In addition, considering the water inventory in the piping from the feed water isolation valve to the steam generator inlet nozzle [1], the relative error of the inventory (+5.6 %) reduces to +1.7 %, which has negligible effects on the transient results. Thus, no further effort has been made for better fitting of the steam generator inventory. Some important data, such as the core inlet flow distribution and exit temperature distributions, are not available. So a detailed comparison of local multi-dimensional flow effects can not be made.

Figure 4 shows the initial steady-state radial power distribution, which is almost symmetric and very similar to that of Exercise II [7]. The resulting effective multiplication factor (k_{eff}) was 1.00580. The radial and axial power distributions are quite flat so that the radial, axial peaking factors, and the axial offset are 1.340, 1.082, and 0.019, respectively.

5.2. Transient Results

The transient begins with simultaneous opening of the break valves at 0.01 sec. Table 2 lists the major sequence of events observed during the simulation. The steam line break causes rapid depressurization in the faulted-loop steam generator and, in turn, a rapid cooling of the primary coolant system. Figures 5 and 6 show the break flow and the steam generator inventory behaviors, respectively. The break flows become null at ~ 80 sec when the faulted-loop steam generator empties. The temporary increase noted in the steam generator inventories is due to the influx of the feedwater existing between the feedwater isolation valve and the steam generator inlet nozzle. Figure 7 shows that the depressurization of the faulted-loop steam generator continues until it completely empties. Meanwhile, the intact steam generator remains

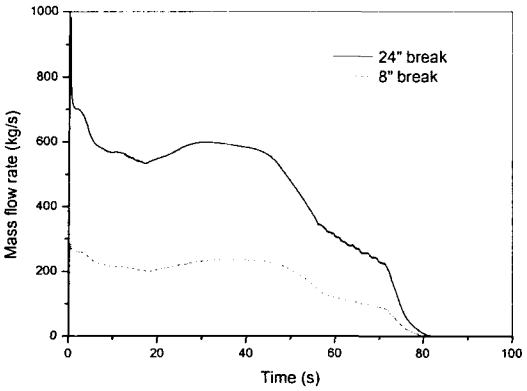

Fig. 5. Break Flow Behaviors

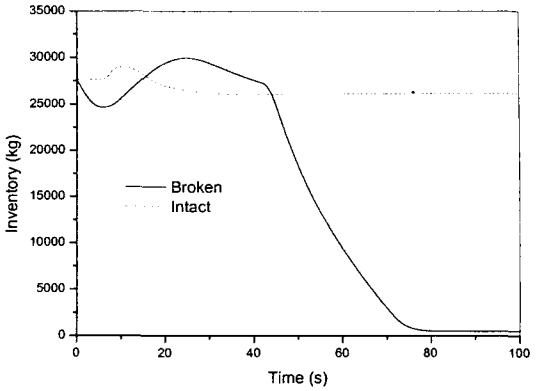

Fig. 6. Steam Generator Water Inventory Behaviors

above 5.9 MPa throughout the transient, because both the feed water and the main steam isolation valves are closed right after the reactor trip.

The asymmetry affects the primary coolant temperatures as shown in Figure 8; the temperature difference between the cold and the hot leg is high in the faulted-side loop, whereas it is negligible in the intact loop. The asymmetry again results in asymmetric core power shapes as well as asymmetric coolant temperature distributions in the reactor vessel. Note that the two temperature curves of the intact side in Figure 8 cross over around 23 seconds, meaning that the hot leg temperature is lower than the cold leg temperature. There are two reasons for this cross over: heat addition from the intact-loop side steam generator and flow mixing in the vessel. The flow mixing causes a temperature reduction in the intact side because the flow of the intact side is mixed with much cooler flow coming from the faulted side.

This transient is extremely asymmetric as identified in Figures 7 and 8. Thus, the flow of the faulted loop preferentially cools half of the reactor core on the faulted-loop side. If perfect mixing of the loop flows were assumed, it would lead to an unrealistic and non-conservative result. No mixing assumption is also invalid. Figures 9 and 10 show that significant mixing occurs in the downcomer, lower plenum and upper plenum. If no mixing occurred in the downcomer and lower plenum, the coolant densities in cells (9,4) and (12,4) should have been represented by "dash-dot" and "dash-dot-dot" lines in Figure 9, respectively. If perfect mixing occurred, the densities in cells (9,4) and (12,4) would have been indicated by a "solid" line in Figure 9. This clearly illustrates that flow mixing is not negligible, especially in the intact-loop side of the lower plenum and downcomer. Figure 10 also shows that more mixing occurs at the upper plenum of the intact side. Without mixing, the up-triangle symbol in Fig. 10 should have been in the right-hand side of the square symbol.

The flow mixing under a forced convection flow can be predicted even with a conventional 1D approach by some extent provided that the reactor vessel is modeled using two equal parallel flow paths by splitting the downcomer, the lower plenum, the core, and the upper plenum [9]. However, it is expected that a 3D flow representation as employed in MARS would result in much better predictions of the mixing because of more realistic treatment of the momentum

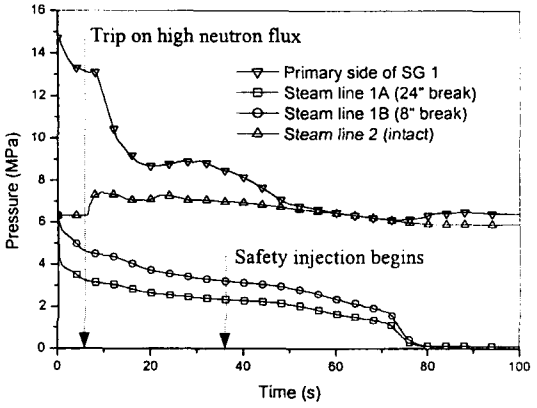

Fig. 7. Pressure Behaviors

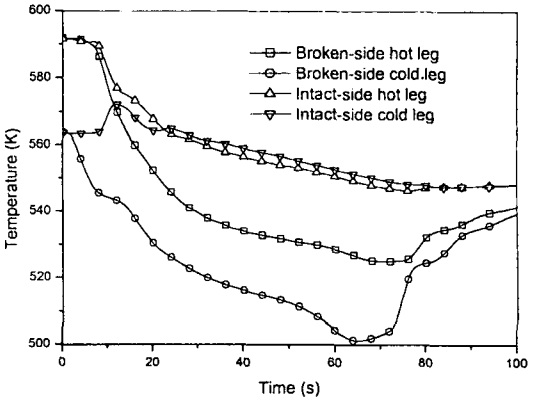

Fig. 8. Coolant Temperature Behaviors

convection terms, especially when the coolant pumps are tripped. Although the degree of flow mixing might not dictate the global core response, it certainly has considerable effects on the power distribution and the local flow phenomena. In this regard, the 3D T/H calculation feature of MARS is considered important.

Figures 11 and 12 show the reactivity and the total core power behaviors, respectively. After the MSLB occurs, the RCS pressure decreases because of the rapid cool down of the primary side. This entails a sudden expansion of core coolant, resulting in a negative reactivity insertion. Thus, for ~3 seconds after the break, the total core power reduces to ~95 %. Then the positive reactivity insertion due to the lowered coolant temperature, however, brings the core power up until the scram occurs. When the core power reaches 114 % of the rated power at 5.96 sec, the reactor trip signal occurs and the control rods begin to be inserted after the 0.4 second delay. The core power then decreases to a level determined by the delayed neutrons generated from the longest living precursor and by the decay heat sources. The core power increases again from ~17 seconds due to the positive reactivity effect by the continued decrease in coolant temperatures. The peak power of 908.1 MW (32.8 % of full power) occurs at 67.2 sec. When the faulted-loop steam generator nearly empties, the primary coolant temperature starts to increase and consequently the core power decreases. The reactivity plot given in Figure 11 shows that the core returns to criticality for a very short period of time.

Figure 13 shows the radial power distribution obtained at the time of maximum core power, 67.2 sec. It is clearly shown that significantly higher power is generated in one half of the core. There are two reasons for the localized power distribution: the asymmetric inlet flow condition and the presence of the stuck rod. Note that the stuck rod was placed intentionally at the faulted side half of the core. Due to this combined effect, the "radial" power peak factor is as high as 3.57.

The consequences of the localized power distribution appear in the local power generation rate which is shown in Figure 14. The curve represents the normalized core power times the assembly-wise 3D peaking factor. As shown in the figure, the peak local power at the time of the maximum core power is over 2.5, which is much larger than the initial state value. Since the pin peaking is even higher than this value and the core

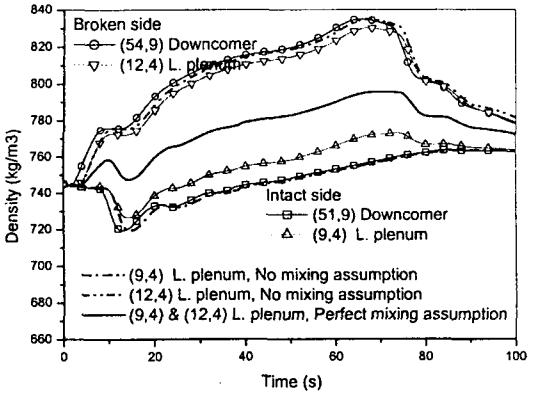

Fig. 9. Water Densities at Downcomer and Core Inlet (i,j)=channel no. j=vertical mesh no

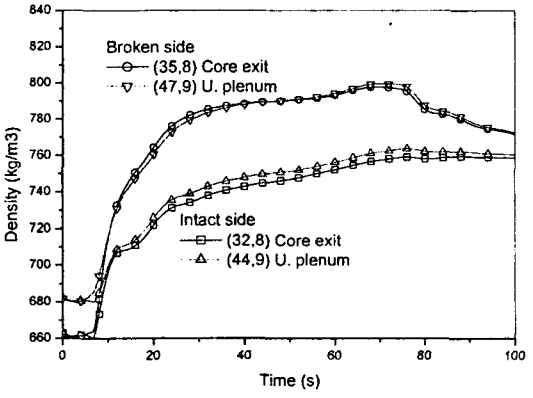

Fig. 10. Water Densities at Core Exit and Upper Plenum (i,j)=channel no. j=vertical mesh no

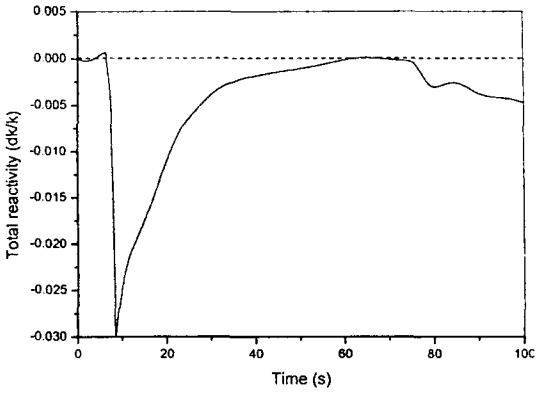

Fig. 11. Total Reactivity Behavior

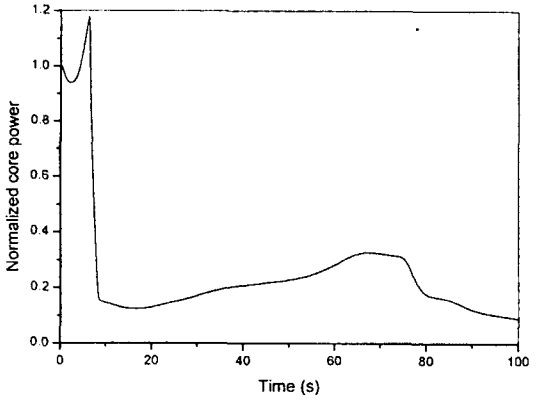

Fig. 12. Total Core Power Behavior

pressure at this time period is only about half of the initial pressure, one can imagine that fuel failure would be a serious safety concern. Note that this kind of observation of the localized phenomena would have not been possible with the lower dimensional kinetics (point or 1D) and, thus, Figure 14 demonstrates one of the most important benefits of using a coupled code such as MARS/MASTER.

In Figure 15, the core power behaviors obtained by the benchmark participants are compared. These graphs were reproduced from Reference 8. It should be noted the data are not the final ones, but the preliminary results. In other words, these are the results of the real blind calculations that have not been affected by each other. However, it can be seen that the MARS/MASTER solution is in the middle of the band and it is very close to the solutions of two participants (marked with "circle" and "triangle" symbols), whose Exercise II results are evaluated to be the most realistic. The close agreement with these solutions is considered remarkable because these were generated independently using different models as well as codes. The comparison confirms the accuracy of the MARS/MASTER solution.

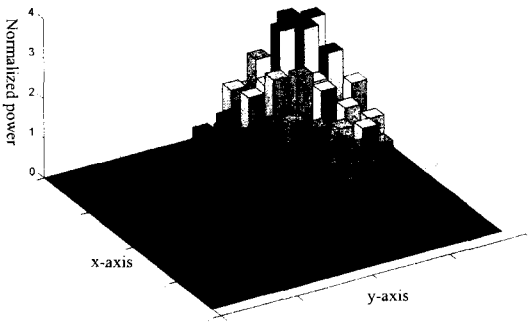

Fig. 13. Radial Power Distribution at 67.2s (when the peak power occurs)

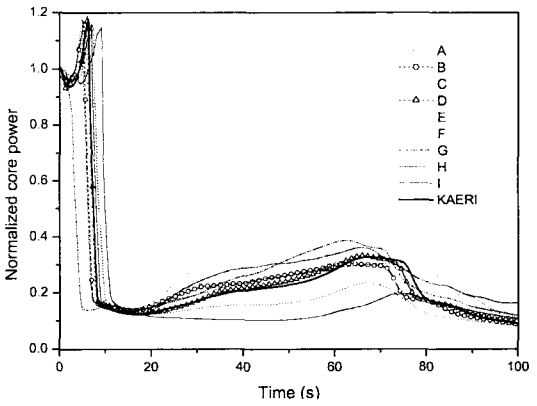

Fig. 15. Comparison of Normalized Core Powers Obtained by the Benchmark Participants

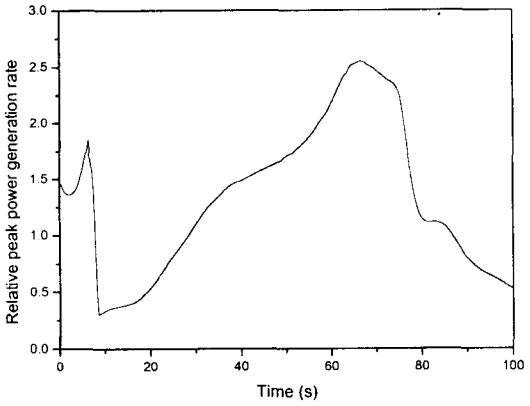

Fig. 14. Evolution of the Peak Power Generation Rate During the Transient

5.3. Computational Speed

This calculation was performed on a personal computer equipped with a 330 MHz Pentium II processor. For the 100-sec transient calculation, it took about 5900 sec, of which ~13 % was used for the kinetics calculation by MASTER and the rest consumed by MARS.

6. Summary and Conclusions

The OECD MSLB Exercise III problem was analyzed using the MARS/MASTER code. The modeling was performed with emphases on the three-dimensional representation of the flow as well as the neutron flux. The results showed that a significant amount of flow mixing occurs in the lower and upper plenum regions under highly asymmetric flow conditions. Regarding the local core power behavior, the code predicts a severe local power peaking of about 2.5 at the time of the maximum-return-to-power which might lead to a fuel failure concern. Comparison of the total core power response with the other participants' solutions confirmed that the MARS/MASTER solution is quite accurate. It also implies that MARS properly predicts the flow mixing in the reactor vessel. In conclusion, the performance of the MARS/MASTER code demonstrated by this complicated benchmark calculation is judged acceptable in terms of both solution accuracy and computational speed.

Acknowledgement

This work has been performed as a part of the Nuclear R&D Program supported by Ministry of Science and Technology (MOST)

References

1. Ivanov, K., Beam, T., and Baratta, A., "PWR MSLB Benchmark, Final Specifications," NEA/NSC/DOC(99)8, OECD Nuclear Energy Agency (April 1999).
2. Lee, W. J. *et al.*, "Development of a Multi-Dimensional Realistic Thermal-Hydraulic System Analysis Code, MARS 1.3 and its Verification," KAERI/TR-1108/98, Korea Atomic Energy Research Institute (1998).
3. Jeong, J.-J., Ha, K.S., Chung, B.D. and Lee, W.J., "Development of A Multi-dimensional Thermal-Hydraulic System Code, MARS 1.3.1," *Annals of Nuclear Energy*, vol. 26, no. 18, pp. 1161-1642 (1999).
4. Lee, W. J. *et al.*, "Improved Features of MARS 1.4 and Verification," KAERI/TR-1386/99, Korea Atomic Energy Research Institute (1999).
5. Cho, B.O. *et al.*, "MASTER-2.0: Multi-purpose Analyzer for Static and Transient Effects of Reactors," KAERI/TR-1211/99, Korea Atomic Energy Research Institute, (Jan 1999).
6. Jeong, J.-J., Joo, H.G. *et al.*, "Development of a Draft Version of MARS/MASTER; A Coupled Code of MARS 1.3 and MASTER 2.0," *Proc. Korean Nucl. Soc. Fall Mtg.*, Seoul, Korea, Oct. 30 - 31, 1998, p. 157 (Paper 86 in CDROM) (1998).
7. Joo, H.G. Cho, B.O, Yoo, Y.J. and Zee, S.-Q. "Analysis of OECD MSLB Benchmark Exercise II using the MASTER Code," *Proc. Int. Conf. Math. Comp. Reac. Phys. Env. Anal. Nucl. Appl.*, Madrid, Spain, Sept. 27-30 (1999).
8. Ivanov, K., Presentation Material for MSLB Exercise III Results Comparison, 4-th Workshop for OECD PWR MSLB Benchmark, Paris, France, Jan. 24 - 25, 2000.
9. Peterson, C.E., et al., "Main-Steam-Line-Break Analysis of TMI-1 using RETRAN-3D", Nuclear Technology, v ol. 128, pp. 233-244 (1999).